

# Computation analysis and optimal design of a high speed response and low power micro valve

Dong Soo Kim\*, Sang Woon Park\*, Hyun Sub Kim\* and Jae Sub Yoo\*

\* IT Machinery Research Center, Korea Institute of Machinery & Materials  
171 Jang-Dong, Yuseong-Gu, Daejeon, Korea  
(E-mail: kds671@kimm.re.kr)

## ABSTRACT

This study was conducted to analyze the special quality of a very low power consumption type of pneumatic on-off micro valve, and to numerically investigate its flow characteristic depending upon a change in stroke. As a result, it was identified that an enough electromagnetic force (2.4N) acted on the solenoid so that the poppet of the micro valve might run a stroke (0.3 mm) at the high response speed (5ms), and that the yoke caused no magnetic force to be emitted. It was identified that the dynamic pressure acting on the poppet wall was little reduced when the poppet stroke was 0.4 mm or less, but that as it got to be beyond 0.4 mm, it was remarkably reduced and when it was 0.8 mm, it went down to 40%.

## KEY WORDS

Micro valve, Poppet, Solenoid, Plunger, Stationary core

## NOMENCLATURE

$F$  : magnetic force  
 $B_g$  : magnetic flux density  
 $S$  : section area of a plunger  
 $m$  : number of coil layers  
 $N$  : number of coil turns  
 $h$  : coil height  
 $\mu_0$  : magnetic permeability  
 $\rho$  : flow resistivity  
 $\xi$  : space factor  
 $d$  : coil diameter  
 $\lambda$  : coil height

## 1. INTRODUCTION

A remarkable development in computer and control technologies enables users to control a micro valve precisely, and so it is widely applied to various fields such as semiconductor chip mounter, production line of electronic products, automatic feeding line of bearing, injection molding machine, fatigue and vibration tester, and so on. It has been recently highlighted as a key technology in development of a technology-intensive process in the semiconductor industry and the like.

The micro valve has an excellent high-speed and repetitive operability, and makes a pressure act on a dynamic area of the poppet uniformly and shows the high responsiveness irrespective of a change in the pressure applied to the port.

The purpose of this study is to design and analyze a very low power consumption type of pneumatic on-off micro valve which has the characteristics of high

responsiveness and very low power consumption. Thereby, this study is to verify its performance. We analyzed a magnetic field of the solenoid and a flow of the poppet by using commercial software (Maxwell and Fluent). As a result, we could verify the performance of the designed micro valve. We plan to ensure optimum design data through future experiments

## 2. DESIGN OF MICRO VALVE

### 2.1 Composition and Operation Principle of Micro Valve

Fig. 1 shows the schematic diagram of the micro valve. The micro valve comprises a poppet valve, a plunger, a stationary core and a spring for controlling the direction of compressed air, and an O-ring and a gasket for intercepting any leakage, and others.

The operation principle of the micro valve is as follows: When the solenoid is electrified, a magnetic force forces the poppet valve to move forward, and thereby, the compressed air flows into a pressure port through a supply port. When the solenoid is not electrified, a spring force forces the poppet valve to move back and thereby, a supply port gets to be closed and the compressed air is exhausted out of an exhaust port. Thereby, it reciprocates at a high speed.

### 2.2 Design Specifications of Micro Valve

Table 1 shows the design specifications and specifications for performance of the micro valve. Specifications for performance are 24VDC in supply power and 3 mm in diameter.

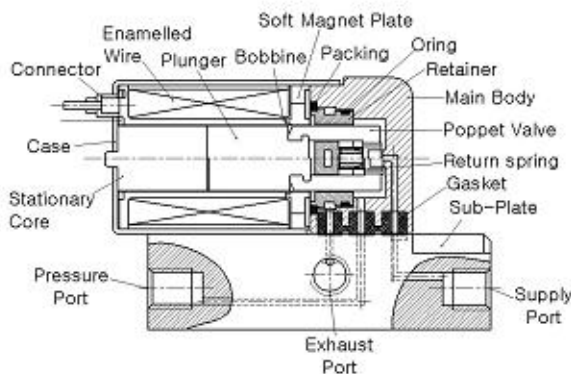


Fig. 1. Schematic Diagram of Micro Valve

Table 1. Design Specifications

Item	Value	Unit
Supply Pressure	3	bar
Supply Voltage	24	V
Electric Power	0.3	W
Port	3	mm
Stroke	0.3	mm
Coil Turn Number	6,200	turn
Coil Diameter	0.04	mm
Coil Resistance	1.5	kΩ
Effective Area	0.19	mm <sup>2</sup>
Flow coefficient	0.01	-
Response Time	10	ms
Temperature Rise Value	50	°C
Magnetic Force	2.4	N
Spring Constant	0.015	N/mm

Design specifications are 0.3W, responsiveness of 10ms or less, compactness of 7 mm in thickness, and low noise of 40dB or below. It is, therefore, characteristically used for the medical purpose.

## 3. ANALYSIS OF MAGNETIC FIELD OF ON-OFF SOLENOID

### 3.1 Design Theory of Solenoid

The key technologies of the micro valve as designed and manufactured are classified into the solenoid technology and the poppet technology. In the case of the solenoid technology, analysis of the magnetic field is important. The magnetic force (F) generated by the solenoid is represented by Equation (1).<sup>4)</sup>

$$F = \frac{B_r^2 S}{2\mu_0} = \frac{10^7}{8\pi} B_r^2 S \quad [N] \quad (1)$$

Where in,  $B_r$  is the magnetic flux density brought about by a permanent magnet and  $\mu_0$  is the magnetic permeability. If S, a section area of the plunger is obtained from Equation (1), it is induced by Equation (2):

$$S = \frac{8\pi \times 10^7 \cdot F}{B_r^2} \quad [m^2] \quad (2)$$

The radius of the plunger is represented by  $r_1 = \sqrt{(2\mu_0 F) / \pi B_e^2}$  and the magneto motive force (U) is induced by Equation (3).

$$U = NI = \frac{B l_v}{\mu_0} + \sum H l_i \quad [A] \quad (3)$$

Then, h and T, which determine a coil space, are determined by Equation (4) as represented by  $\theta_v$  and which are values by  $\theta_f$  which the temperature is increased.

$$\begin{aligned} \theta_v &= (I^2 R) / (2\lambda l_\pi h) \quad [^\circ C] \\ \theta_f &= (q\rho / 2\lambda\xi T) \cdot (NI / h)^2 \quad [^\circ C] \end{aligned} \quad (4)$$

Wherein,  $\theta_v$  is the value by which the final temperature is increased, and  $\theta_f$  is the value by which a continuous specific temperature is increased, and T is the coil width (h /  $\beta$ ).

If h (coil height) is obtained from Equation (4), it is induced by Equation (5):

$$h = \sqrt[3]{\frac{q\beta\rho U^2}{2\lambda\xi\theta_f}} \quad (5)$$

Wherein, q is the rated time,  $\rho$  is the flow resistivity,  $\lambda$  is the heat dissipation coefficient of the coil, and  $\xi$  is the space factor of winding

Then, the inner diameter/outer diameter ( $r_1', r_2'$ ) of the coil should be determined. The inner diameter ( $r_1'$ ) is determined by the outer diameter of the plunger + the coil polarity + the bobbin thickness. From  $r_2' + r_1' + T$  and  $V = IR$ , the voltage expression, Equation (6) is induced:

$$V = \frac{4\rho(r_1' + r_2')NI}{d^2} \quad [V] \quad (6)$$

Therefore, the coil diameter (d) can be obtained as in Equation (7).

$$d = \sqrt[3]{4\rho(r_1' + r_2') \frac{NI}{V}} \quad [mm] \quad (7)$$

Accordingly, the number of coil layers is determined by  $m = T / d$ , and the number of windings is determined by  $N = ((h / d) - 1)m$ .

For an increase in temperature, the exciting current ( $I_a$ ) should be obtained in the first place. The mean length ( $l_\pi$ ) and full length ( $l_f$ ) of the coil are as in Equation (8).

$$l_\pi = \pi(2r_1 + T), \quad l_f = M_\pi \quad (8)$$

Coil resistance (20°C) =  $l_f \times$  resistance coefficient,  
Coil resistance (100°C) =  $1.314 \times R_c$ ; Exciting current ( $I_a$ ) =  $V / R_{th}$ ; and magneto motive force (U) =  $NI_b$ . Therefore, an increase in the temperature is determined by  $\theta_f$ .

### 3.2 Solenoid Modeling and Result of Analysis thereof

In order to analyze the solenoid part of the micro valve, the solenoid is modeled as shown in Fig. 2. The analysis results including the response characteristic of the micro valve depending upon the solenoid are shown in Figs. 2~ 5.

As can be known from Figs. 2~ 9, it can be known that an enough electromagnetic force (2.4N) is working so that a displacement (0.3 mm) in which the micro valve moves may take place. They show characteristics of the high-speed position responsiveness and the speed responsiveness.

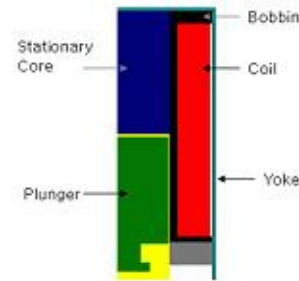


Fig. 2 Modeling of Solenoid

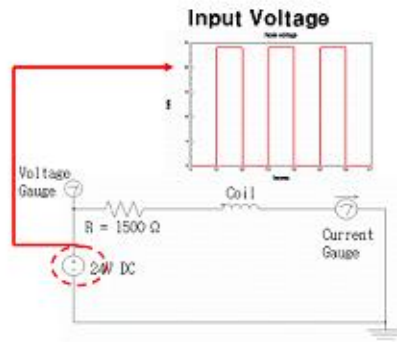


Fig. 3 Schematic Diagram of Solenoid Circuits

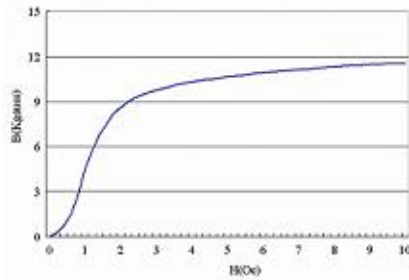


Fig. 4 B-H Curve of Material

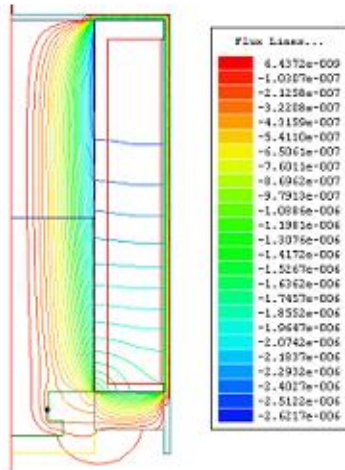


Fig. 5 Flux Contour of Solenoid

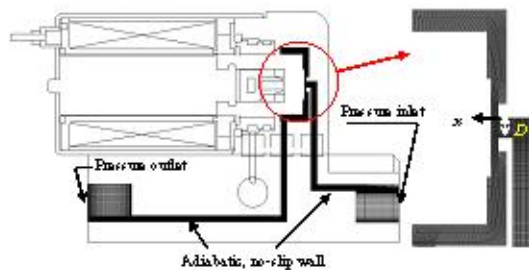


Fig. 6 Schematic diagram and grid system used in numerical computation

## 4. NUMERICAL ANALYSIS OF THE FLOW FIELD OF THE POPPET

### 4.1 Calculation Area and Boundary Conditions

In order to grasp the flow field characteristic in the micro valve, the flow field of the poppet was analyzed by changing the pressure ratio between upstream and downstream in the flow field and the poppet stroke. Fig. 6 shows the calculation area and the grid system used in numerical computation. Air (the ratio of specific heat is 1.4) was used as an operating fluid in numerical computation. Pressure inlet conditions were applied to the inlet boundary, pressure output conditions were applied to the outlet boundary, and adiabatic no-slip conditions were applied to the wall. The upstream supply pressure ( $P_0$ ) was fixed at 0.3MPa and the outlet pressure ( $P_b$ ) was set at the atmospheric pressure. Then the flow field of the poppet was numerically analyzed by changing the dimensionless length to 0.2, 0.4, 0.6 and 0.8 in 4 phases with respect to the maximum stroke of the poppet. The range of the poppet stroke displacement is  $0 \leq x \leq 0.438$ .

The alignment grid system was used in numerical computation and it generated about 40,000 node points. Also, in order to simulate properly development of boundary layers by viscosity on the wall and the flow field in the minimum area, grids were concentrated on the wall and the minimum sectional area.

### 4.2 Dominant Equation

In numerical computation, compressive Navier-Stokes equations as follows were used. In order to simulate properly the effect of turbulence on the flow field in the micro valve, a standard  $k-\varepsilon$  turbulent model was used, which was an eddy viscosity model using the Boussinesq hypothesis<sup>12)</sup>.

$$\frac{\partial \rho}{\partial t} + \frac{\partial (\rho u_i)}{\partial x_i} \quad (9)$$

$$\frac{\partial}{\partial t} (\rho u_i) + \frac{\partial}{\partial x_j} (\rho u_i u_j) = \frac{\partial}{\partial x_j} \mu \left( \frac{\partial u_i}{\partial x_j} + \frac{\partial u_j}{\partial x_i} \right) - \frac{\partial}{\partial x_i} \left( \frac{2}{3} \mu \frac{\partial u_i}{\partial x_i} \right) - \frac{\partial p}{\partial x_i} + \frac{\partial}{\partial x_j} (-\rho \overline{u_i u_j}) \quad (10)$$

Equations (9), (10), and (11) were made to be discrete by FVM (finite volume method). The upwind scheme was applied to the space term and the 4-phase Runge-Kutta method was applied to the time term. For convergence determination of a solution, a residual difference in each state quantity was set at  $10^{-4}$ . We investigated the change of the mass flow at the inlet

and outlet of the flow field and then the condition in which the sum of the mass flow was 0.3% or less was set as the convergence condition.<sup>1)</sup>

$$\frac{\partial}{\partial x}(\rho E) + \frac{\partial}{\partial x_i}(\rho u_i H) = \frac{\partial}{\partial x_i} \left[ \left( x + \frac{\mu_i}{Pr_i} \frac{\partial T}{\partial x_i} + u_i (\tau_{ij})_{eff} \right) \right] \quad (11)$$

### 4.3 Result and Review of Numerical Analysis

Fig. 7 shows the velocity vector and the Mach number at the point in which the poppet strokes against the maximum displacement of the poppet is 0.2. At the point that the sectional area gets to be minimum as the poppet approaches to the flow outlet, fluid passes through the flow channel with it being accelerated at the supersonic speed. Also, it can be identified that the flow is separated in the lower end of the poppet so that a vortex flow is formed.

Fig. 8 shows the dynamic pressure distribution along the poppet wall. The horizontal axis indicates the position along the poppet wall in a red dotted line to the upper-left part of the graph and the longitudinal axis indicates the dynamic pressure which represents the supply pressure at the dimensionless length.<sup>2,3)</sup> A high distribution of the dynamic pressure is shown in the center of the poppet wall due to the effect of the air as emitted out of a narrow pipeline in the inlet, and it tends to be rapidly reduced beyond the minimum sectional area. Considering the change of dynamic pressure depending upon the poppet stroke, the dynamic pressure is little reduced and a similar value is maintained until  $x/D$  gets to be 0.4, while it is rapidly reduced after  $x/D$  gets to be 0.6. It can be, therefore, known that when  $x/D$  gets to be far, upto 0.8, only 40% of a peak of the dynamic pressure at the initial position acts on the poppet wall.

Fig. 9 shows the velocity vector inside the flow field as obtained by three-dimensional analysis. The incoming fluid from the inlet gets to be accelerated through a narrow pipeline so that as a flow thereof is formed around the poppet, it gets to be spouted to the outlet of the flow field. It can be known that the flow rate is accelerated again as the fluid gets out of the lower end of the poppet and goes down through a pipe of which the sectional area is narrow.

Fig. 10 shows the turbulence intensity inside the flow field. The expected result of the turbulence intensity and the distribution thereof inside the flow field can be identified in it. Also, it can be known that the closer the flow goes to the outlet, the greater the turbulence intensity increases, and particularly that a strong turbulence intensity is shown in the point where the flow is turned.

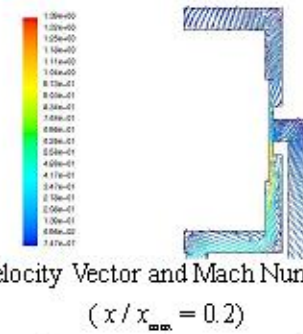


Fig. 7 Velocity Vector and Mach Number (color)  
( $x/x_{max} = 0.2$ )

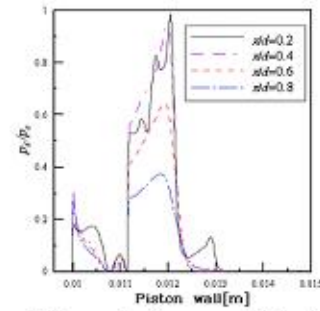


Fig. 8 Dynamic Pressure Distribution along the Poppet

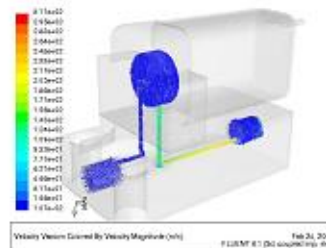


Fig. 9 Valve Interior Flow Chapter Velocity Vector

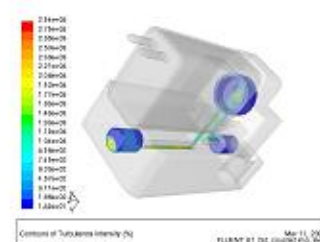


Fig. 10 Turbulence Intensity of Flow Field



Fig. 11 Micro Valve Parts

## 5. TEST ON MICRO VALVE

Fig. 11 shows components of the micro valve and Fig. 12 shows a performance test device for the micro valve. In order to measure the flow capacity of the developed micro valve, it was tested by opening it with the

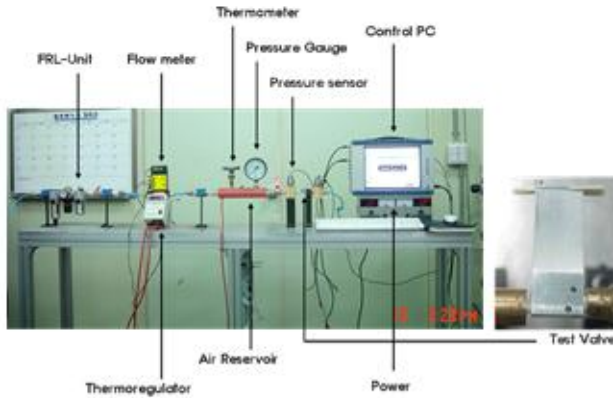


Fig. 12 Performance Test Device

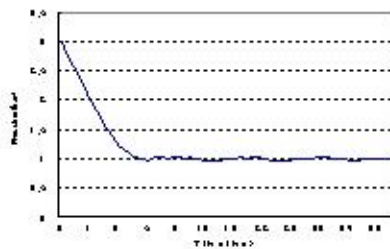


Fig. 13 Flow Coefficient Test

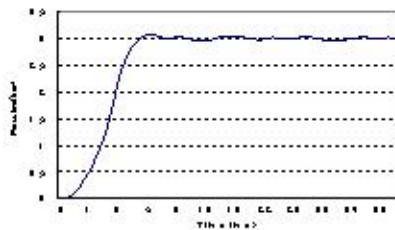


Fig. 14 Response Test

operating pressure set at  $3 \text{ kg/cm}^2$  until the operating pressure gets to be  $1 \text{ kg/cm}^2$ . The result is shown in Fig.13. Also, in order to measure the response characteristic of the micro valve, it was tested by applying voltage to the valve so that it may be on from off until the operating pressure gets to be  $3 \text{ kg/cm}^2$  from  $0 \text{ kg/cm}^2$ . The result is shown in Fig. 14. As can be known from the test results, it was identified that the flow capacity coefficient ( $C_v$ ) of the developed micro valve was 0.01 and the dynamic response time was 5msec (at 3bar).

## 6. CONCLUSION

In this study, the performance of the micro valve was evaluated through analysis of the characteristics of the very low power consumption type of pneumatic on-off micro valve and test thereof, and thereby, the following results were obtained;

1. It was identified that an enough electromagnetic

force (2.4N) acted on the solenoid so that the poppet of the micro valve might run a stroke (0.3 mm) at the high response speed (5ms), and that the yoke caused no magnetic force to be emitted.

2. The characteristics inside the flow field depending upon a change of the poppet stroke were numerically analyzed. As a result, the velocity vector field and the pressure field inside the micro valve were properly simulated. Also, it was identified that the dynamic pressure acting on the poppet wall was little reduced when the poppet stroke was 0.4 mm or less, but that as it got to be beyond 0.4 mm, it was remarkably reduced and when it was 0.8 mm, it went down to 40%. This means that the flow capacity coefficient indicating the effective sectional area of the micro valve is 0.01.

3. The micro valve was manufactured and further tested in order to verify its performance by using a performance test device. The test results showed the winding current (16mA), the electric power (0.3W), the flow capacity coefficient (0.01), the effective area ( $0.19 \text{ mm}^2$ ), and response time(5ms). The performance test and the analysis thereof demonstrated that the optimum design of the micro valve was feasible.

## ACKNOWLEDGEMENTS

This study was performed under the program of "Development of a Very Low Power Consumption Type of Micro Valve" sponsored by the Ministry of Commerce, Industry and Energy. We thank all persons concerned from the bottom of our heart.

## REFERENCE

1. B. W. Andersen, "The Analysis and Design of Pneumatic Systems", John Wiley & Son Inc., pp. 48~61, 1967.
2. W. L. Green, "The Poppet Valve-Flow Force Compensation," Proceedings of Fluid Power International conference, pp. S1-S6, 1970.
3. K. Kakano, H. Watanabe and G. Mao-ving, "Experimental Study for the Compensation of Axial Flow Force in a Spool Valve", Journal of the Japan Fluid Power System Society, Vol. 18, No. 6, pp. 475~482, 2000.
4. 中田 高儀, "有限尿素法による 交直電磁石の設計と應用", 森北出版株式会社, pp. 63~90, 1991.